IEEE Access
Multidisciplinary ⋮ Rapid Review ⋮ Open Access Journal

Received March 7, 2022, accepted March 18, 2022, date of publication March 28, 2022, date of current version April 1, 2022.

Digital Object Identifier 10.1109/ACCESS.2022.3162618

Dynamic Algorithm for Interference Mitigation Between Cells in Networks Operating in the 250 MHz Band

DICK CARRILLO MELGAREJO[1,2], (Member, IEEE), LUIZ QUIRINO REZENDE DA COSTA FILHO[3], ÁLVARO AUGUSTO MACHADO DE MEDEIROS[3,4], CARLOS LORENA NETO[5], FABRICIO LIRA FIGUEIREDO[6], AND DEMÓSTENES ZEGARRA RODRÍGUEZ[7], (Senior Member, IEEE)

[1]Department of Electrical Engineering, School of Energy Systems, Lappeenranta-Lahti University of Technology (LUT), 53850 Lappeenranta, Finland
[2]School of Electrical and Computer Engineering, State University of Campinas, Campinas 13083-970, Brazil
[3]Department of Electrical Engineering, Federal University of Juiz de Fora University (UFJF), Juiz de Fora 36036-900, Brazil
[4]Department of Computer Science, Munster Technological University, Cork, T12 P928 Ireland
[5]Tropico Systems and Telecommunications, Campinas 13086-510, Brazil
[6]Research and Development Center in Telecommunications (CPqD), Campinas 13086-902, Brazil
[7]Department of Computer Science, Universidade Federal de Lavras (UFLA), Lavras 37200-000, Brazil

Corresponding author: Dick Carrillo Melgarejo (dick.carrillo.melgarejo@lut.fi)

This work was supported in part by the Academy of Finland through FIREMAN Consortium under Grant CHIST-ERA-17-BDSI-003 and Grant 326270, in part by the EnergyNet Research Fellowship under Grant 321265 and Grant 328869, and in part by the Jane and Aatos Erkko Foundation through STREAM Project.

ABSTRACT The growing demand for Internet of Things (IoT) applications in agribusiness increases the necessity of reliable and secure connectivity in rural areas. Thus, in the particular case of Brazil, some initiatives aim to take advantage of frequency bands dedicated to limited private services. For instance, cellular networks based on orthogonal frequency-division multiple access (OFDMA) in 250 MHz bands require specialized adaptations because the interference between cells increases when these systems operate in the Very High Frequency (VHF) band. This work presents an analysis based on a reliable simulation of interference mitigation in OFDMA systems at 250 MHz using a network simulator. The simulator is calibrated with data obtained in the field by an extensive and rigorous drive test. Therefore, the analysis is based on a comparison of traditional frequency reuse schemes with a machine learning approach based on deep reinforcement learning (DRL) to reduce inter-cell interference. The numerical results indicate that the DRL approach outperforms the traditional frequency reuse (FR) schemes in four different typical agribusiness scenarios.

INDEX TERMS Frequency reuse, Internet of Things, deep reinforcement learning, customized cellular networks, 250 MHz.

I. INTRODUCTION

The Internet of Things (IoT) is an emerging and promising technology that aims to revolutionize the world through the connection of every physical object to the Internet. Although the IoT concept is generic, involving Internet connections in highly dense urban areas for a diversity of applications, many solutions are being developed for use in rural areas to support applications that today are being prioritized by the pandemic [1] (remote education, remote working, and remote healthcare), and also the agribusiness market [2]. Thus, relevant characteristics of rural regions, such as difficult access and long distances involved, have a direct impact on the development of IoT solutions for pandemic [3] and agribusiness scenarios [4]. Unfortunately, most of the technologies offered by telecom operators in urban areas are not available in remote areas, which makes it difficult to use adequate transport layer technologies to support IoT applications. Therefore, the use of very high frequency (VHF) bands is emerging as a technical solution to improve the propagation and optimize the coverage of wireless communication systems [5].

The associate editor coordinating the review of this manuscript and approving it for publication was Ali Afana.

The increasing connectivity demand in rural areas has driven several research and development projects into designing cellular network solutions for this specific scenario. Several wireless technologies are compared in [6] to provide Internet access in rural areas. Long-Term Evolution (LTE) arises as a solution that can provide a variety of services for rural IoT environments. For instance, the feasibility of an LTE network in the 800 MHz frequency band to serve rural areas in India and Spain is presented in [7] and [8]. The details of planning an LTE network operating in the 900 and 1800 MHz frequency bands in Indonesia are presented in [9]. In [10], the coverage and capacity of LTE IoT technologies, namely LTE machine-type communication (LTE-M) and narrowband IoT (NB-IoT), are analyzed in Denmark through an intensive drive test with the network operating in the 800 MHz frequency band. In [11], a Fourth Generation (4G) network is analyzed in the field in order to identify gaps that aim to be supported by Fifth Generation (5G) in rural scenarios.

One important drawback of using cellular networks in sub-1GHz bands, such as 250 MHz, is the inter-cell interference. To address this issue, in [12], a flexible tool was provided to implement traditional FR schemes in the LTE. Details of these FR techniques are described in a comprehensive survey of inter-cell interference coordination (ICIC) techniques in [13]. These techniques aim to improve the basic FR concept to mitigate or avoid interference between cells. As the FR evolves from a static to a dynamic procedure, the ICIC algorithm complexity increases such as typical resource allocation algorithms [14]. Such an increase in complexity requires higher processing capabilities of the base station, thereby having an impact on the final cost. This may not be an issue when a dense urban scenario is considered, where cells become smaller in order to meet the increasing demands of the traffic of a large number of users [15]–[17]. However, when it comes to a rural scenario, the extensive coverage requirements and the sparse user occupation of the cell discourage the cellular network deployment. Thus, there is a demand for simple and cheaper solutions that will not bring a significant increase in the operational and capital expenditures (OPEX/CAPEX) of IoT network providers [5], [18].

Recently, artificial intelligence methodologies for cellular network optimization have been gaining popularity. Especially in radio resource management, the allocation of resources is a difficult task. For instance, in [19], a deep reinforcement learning-based decentralized multiagent power control algorithm was proposed to improve the sum rate of a cellular network. In [20], multiagent deep reinforcement learning-based autonomous channel selection and transmission power selection were used to reduce the co-channel interference in a cellular network. However, to the best of author's knowledge, there is no similar approach with a proper comparison of traditional FR schemes with this deep reinforcement learning approach, especially in 250 MHz bands.

One of the primary motivations of this study is to compare the performance of traditional FR schemes with radio resource scheduling allocation based on deep reinforcement learning.

To establish the framework of our study, we provide a brief contextualization of the problem and a description of the particular scenario in Brazil and highlight the main contributions of this paper in the following subsections.

A. PROBLEM CONTEXTUALIZATION

As the rural scenario requires an extensive area cell coverage, the operation in a lower frequency band can make the provision of IoT services feasible for many agribusiness applications, such as precision farming, livestock control, storage monitoring, and automation of agricultural processes. However, the usage of lower frequency bands also implies higher inter-cell interference. An advanced solution is the use of directional antennas aimed at narrowing the radiation lobe of each sector and reducing the secondary lobes [21]. However, because of the low availability of off-the-shelf directional antennas for this frequency range, spectrum allocation and channel reuse control techniques, such as ICIC techniques, stand out as a viable solution for performance improvement in a VHF propagation scenario.

As the orthogonal frequency division multiplexing access (OFDMA) allows more specific occupation of the spectrum on a shorter time basis, the allocation management of resources for each user in the cell can be optimized in order to reduce the interference between cells. In such a way, a minimum quality of service (QoS) can be reached in different regions of the cell after applying techniques such as FR. Following this assumption, each resource block (RB) can be assigned with a specific transmission power to cell users in different time and space domains to reuse the neighbor cells.

B. THE PARTICULAR SCENARIO IN BRAZIL

In 2010, the Brazilian National Agency of Telecommunications (ANATEL) released Resolution 555 [22], which allocates 225 MHz to 270 MHz to the private limited service (SLP) on a primary and nonexclusive basis, aiming to modernize the radios that occupy this band. In this context, this paper presents a broadband system based on the LTE protocol stack, which was adapted and developed to operate in VHF bands. The target is to provide broadband IoT services to the agribusiness markets, because the coverage of large areas of plantations or pastures is favored by the best propagation in the range of VHF. This broadband technology has shown satisfactory results in terms of the radius of cell coverage and the ability to support several IoT solutions. As the 250 MHz frequency band is not available worldwide for such purposes, there is a lack of studies that analyze the performance of an LTE network in this scenario.

C. CONTRIBUTION

The main contributions of this study are the following:

- An open-source simulator is calibrated with data obtained in a driving test on a real scenario of the

network operating in 250 MHz in Brazil. Thus, our results provide a strong representation of what is expected in real scenarios. (https://gitlab.com/aikonbrasil/freuse250mhz).
- A novel FR is proposed based on a deep reinforcement learning scheme to schedule sub-bands and power transmission simultaneously.
- The performance of typical FR schemes is evaluated and compared with the proposed approach in a cellular network operating in 250 MHz.
- An open source simulator is calibrated with data obtained by a drive test on a real scenario of the network operating in 250 MHz in Brazil. Thus, our results provide a strong representation of what is expected in real scenarios.

With the network simulator already calibrated to simulate real scenarios, we execute a performance analysis of ICIC techniques, presenting improvements in the system, especially in scenarios with high interference. Furthermore, we propose an algorithm that can be easily implemented in the deployed base stations in order to reduce interference considering performance for different scenarios.

The paper is organized as follows. Section II describes the cellular network developed for agribusiness applications that are used to obtain field measurements in 250 MHz. The adaptation of the ns-3 simulator to the field test network is detailed in Section III. Section IV gives a summary of the FR algorithms considered in this study. In Section IV-D, the algorithm proposed in this work is described. Section V provides details of the simulation campaign. In Section VI, the simulation results are presented and discussed. Conclusions and future work are addressed in Section VII.

II. DEPLOYMENT IN A REAL SCENARIO

Resolution 555 of the National Agency of Telecommunications (ANATEL) of Brazil, which allocates the 225 MHz to 270 MHz band to the Private Limited Service (SLP) on a primary and non-exclusive basis [22], was published in 2010 with the intent to modernize the radios operating in this band. In this context, a broadband system was developed based on the LTE to operate at this frequency band to provide broadband IoT services to the agribusiness market because the best propagation range of VHF favors the coverage of large areas of plantations or pastures.

The developed system is based on the protocol stack defined by the 3rd Generation Partnership Project (3GPP) LTE Release 8[1] [23] for the base station (BS) and cellular terminal (User Equipment or UE) software. The developed LTE system operates in the FDD (Frequency Division Duplex) mode, with a 5 MHz bandwidth, within the Resolution 555 bands described in Table 1.

The broadband system operating in the 250 MHz band was installed in a rural area of the interior of São Paulo belonging to a sugarcane plantation. The characteristics of the elements used to assemble this cellular network are described in Table 2.

[1]The same approach also applies to 5G new radio, since it is also based on OFDMA as stated in [11].

TABLE 1. Channeling used in the broadband system operating in the 250 MHz band.

Central Frequency (MHz)	Channels (Based on Res. 555 - ANATEL)	Band
228.75 (Uplink), 251.25 (Downlink)	1,2,3,4,5	A
237.50 (Uplink), 265.00 (Downlink)	7,8,9,10,11	B

TABLE 2. Key features of the broadband system operating in the deployed 250 MHz band.

Element Name/Feature	Quantity / Information
Base station	3 units
UE's (Terminal)	10 units
Frequency Band	Band A
Bandwidth	5 MHz (25 RBs)
Type of duplexing	FDD
BS Antenna Height	40 m
UE Antenna Height	3,5 m
Transmission power of each UE	30 dBm
Transmission power of each BS	43 dBm

A. DEPLOYED BROADBAND SYSTEM ARCHITECTURE

The field installation of the broadband system operating in the 250 MHz band was performed according to the architecture described in Fig. 1. In this Figure, it is possible to differentiate the main components of a cellular network, e.g., the evolved packet core (EPC), which is responsible for managing each user's features, such as charging, QoS, connectivity with external networks, IP packet addressing (Internet Protocol), paging processes, and user authentication. The other elements, installed in the field and taking care of the air interface, are part of the access network. The access network consists of the BS and the user terminal (UE). Note also in Fig. 1 that the UEs were installed on machines that participate in the sugarcane process. It is also possible to identify the network used as backhaul, called point-to-point (P2P) radio, in addition to other technologies used in IoT applications.

B. FIELD MEASUREMENTS

Field measurements were performed considering the topology shown in Fig. 2. In this Figure, it is observed that the distance between the base stations varies between 20 and 24 km. Fig. 2 also indicates the region to most likely present interference between cells.

A field measurement procedure was developed to collect data regarding throughput, signal to interference plus noise ratio (SINR), and system coverage. The system achieved a cell radius up to 40 km with an acceptable SINR value that enabled a data rate up to 2 Mbps (downlink).

III. CALIBRATION OF SIMULATION TOOLS

Because the ns-3 simulator only supports some bands defined by the LTE standard, it was necessary to adapt the EARFCN

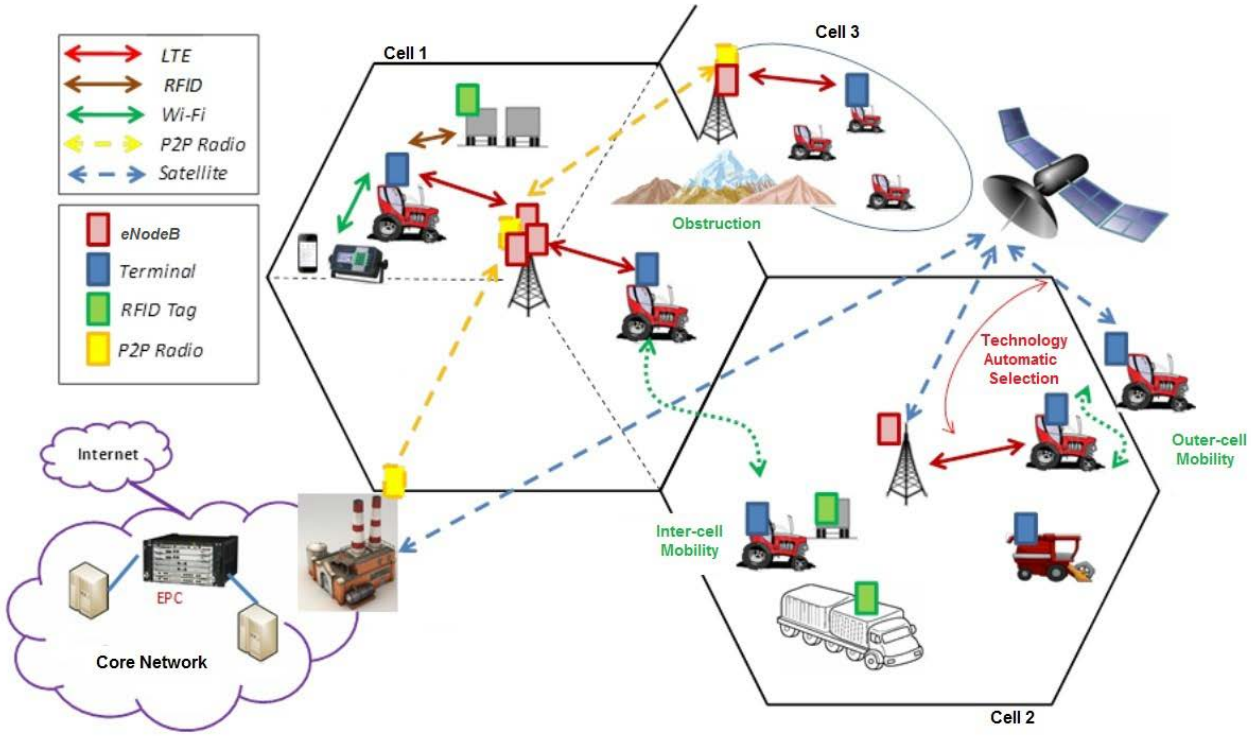

FIGURE 1. Agribusiness architecture deployed in the field using a broadband wireless network based on an OFDMA network, such as the LTE.

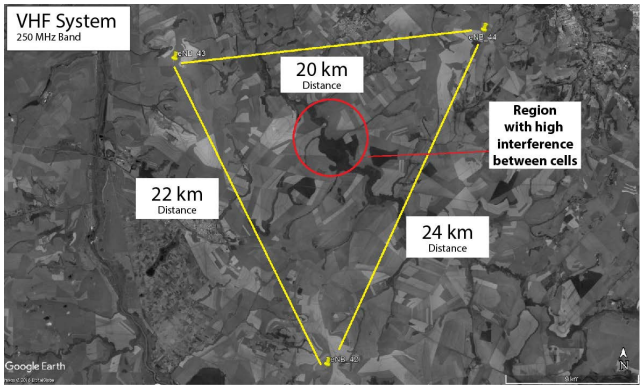

FIGURE 2. Topology of the broadband system operating in the 250 MHz band used for field measurements.

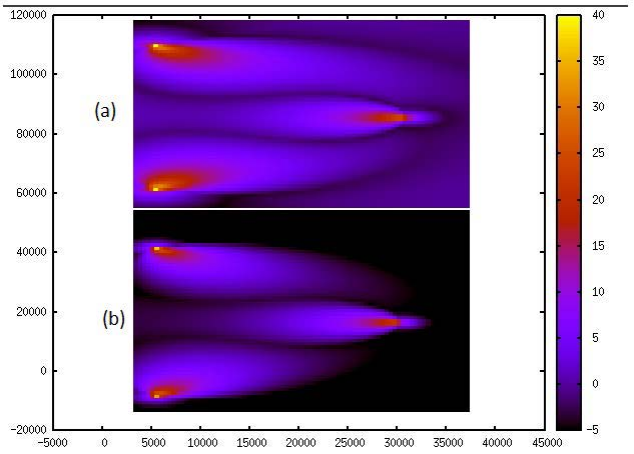

FIGURE 3. Adaptation of the configuration of the ns-3 LTE module to support the 250 MHz band. (a) Signal strength obtained in the ns-3 with EARFCN = 12 modified to operate in the 250 MHz band. (b) Signal strength obtained in the ns-3 with the original EARFCN = 12 operating in the 700 MHz band. The color bar represents the measured signal strength in dBm.

(evolved-UTRA absolute radio frequency number) configuration so that the protocol stack of the simulator considers the propagation calculations of the VHF band. Fig. 3 shows the addition of the coverage of each cell when the system operates in the 250 MHz band in comparison with the operation at 700 MHz (EARFCN=12).

Using the values of the received signal strength indicator (RSSI), SINR, and throughput measured in the field, a calibration was made in the model of large-scale attenuation of the wireless channel used in the simulator. Among the large-scale models defined for the ns-3 simulator, the one that best adapted to the values measured in the field was the Okumura–Hata model [24]. The calibration process consists of altering the parameters of the Okumura–Hata empirical formula so that the values of simulated RSSI, SINR, and throughput are very similar to measurements obtained in the field.

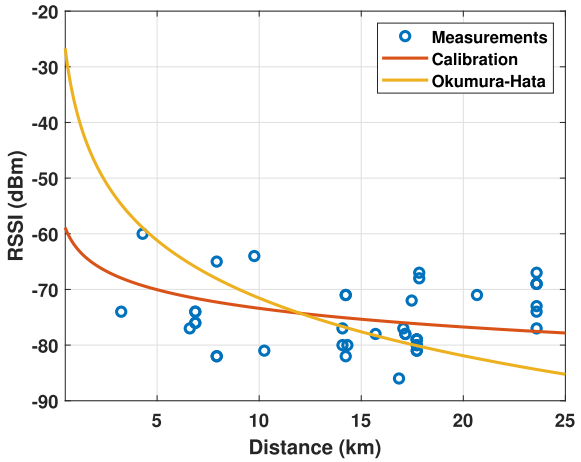

FIGURE 4. Calibration of the modified Okumura–Hata path loss model based on RSSI field measurements.

Signal attenuation in open rural areas in the classical Okumura–Hata formula is given by

$$L = L_{\text{urban}} - 4,78(\log f)^2 + 18,33 \log f - 40,93, \quad (1)$$

where f is the frequency of the transmitted carrier and L_{urban} is the loss given in the urban environment, which, in turn, is calculated by

$$L_{\text{urban}} = 69,55 + 26,16 \log f - 13,82 \log h_t - A(h_r) + (44,9 - 6,55 \log h_t) \log d, \quad (2)$$

where h_t and h_r are the heights of the transmitting and receiving antennas, respectively, $A(h_r)$ is a correction factor as a function of h_r and the size of the city, and d is the distance between the transmitter and the receiver.

Thus, (1) and (2) were altered to fit the values obtained by the field measurements, resulting in

$$L = L_{\text{urban}} - 4,78(\log f)^2 + 18,33 \log f - \mathbf{15,94}, \quad (3)$$

and

$$L_{\text{urban}} = 69,55 + 26,16 \log f - 13,82 \log h_t - A(h_r) + (\mathbf{20,9} - 6,55 \log h_t) \log d, \quad (4)$$

respectively. Table 3 shows the SINR values measured at points of the drive test and those obtained with the ns-3 simulator after the change of the model proposed in (3) and (4).

IV. SYSTEM MODEL AND FREQUENCY REUSE ALGORITHMS

Consider a set $\mathcal{I}$ of I BSs providing downlink wireless service to a group of user equipments (UEs) in a geographical area $\mathcal{A}$. Each BS $i \in \mathcal{I}$ serves an area $\mathcal{A}_i$, such that $\cup_{\forall i \in \mathcal{I}} \mathcal{A}_i = \mathcal{A}$ and $\mathcal{A}_i \cap \mathcal{A}_k \neq \emptyset$ for any $i \neq k \in \mathcal{I}$. In other words, it is possible that some cells have a significant intersection between them. Then, the downlink spectral efficiency achieved by the subchannel m, the user n, at the time slot t from the BS located

TABLE 3. Comparison of the measured values with the values obtained by the simulator after calibration.

Location	SINR Measured	SINR in Simulator
Spot 1	25,5 dB	26,5 dB
Spot 2	23 dB	25 dB
Spot 3	27,8 dB	25 dB

at x_i to a UE located at $y \in \mathcal{A}_i$ is

$$\mathcal{C}^{(t)}_{n,m}(x_i, y) = \log_2 \left(1 + \gamma^{(t)}_{n,m}(x_i, y)\right), \quad (5)$$

where $\gamma^{(t)}_{n,m}(x_i, y)$ is the SINR at the user n, on the subchannel m, at the time slot t, which is defined in (6)

$$\gamma^{(t)}_{n,m}(x_i, y) = \frac{\left[\beta^{(t)}_{l,m}\, g^{(t)}_{l\to n,m}(x_l, y)\, p^{(t)}_l\right]_{l=n}}{\sum\limits_{v \neq l} \beta^{(t)}_{v,m}\, g^{(t)}_{v\to n,m}(x_v, y)\, p^{(t)}_v + \sigma^2_n}, \quad (6)$$

where $\beta^{(t)}_{v,m}$ is the binary variable that indicates the subchannel selection m transmitted from the BS v at the time slot t, $g^{(t)}_{v\to n,m}(x_v, y)$ indicates the downlink channel gain from the BS v to the user n on the subchannel m in the time slot t when the UE is located in the position y and the BS in the position x_v, $p^{(t)}_v$ is the transmit power of the BS v in the time slot t, and σ^2 is the additive white Gaussian noise power spectral density at the user receiver n

$$g^{(t)}_{v\to n,m}(x_v, y_n) = h^{(t)}_{v\to n}(x_v, y_n)\left|\alpha^{(t)}_{n\to l,m}\right|^2, \quad t = 1, 2, \cdots, \quad (7)$$

where $h^{(t)}_{v\to n}(x_v, y_n) = L$ is the path loss on a linear scale, which is calculated in (1), and $\alpha^{(t)}_{n\to l,m}$ is the small-scale Rayleigh fading.

It is important to note that based on this framework, the possibility of using fractional frequency reuse (FFR) is based on the proper definition of the binary variable $\beta^{(t)}_{v,m}$ to choose one specific subchannel or band m, which is used by BS v. Another important parameter considered in FFR schemes is the proper consideration of the power transmission in each BS, which is modeled with the variable $p^{(t)}_v$.

In this work, we implement five methodologies, one methodology based on a deep reinforcement learning approach to define the FR dynamically, and four static algorithms derived from [12].

Based on the system model described before, we define these five methodologies of FR in the following.

A. HARD FREQUENCY REUSE

As in traditional cell reuse, the band is divided into N subchannels, and each of the neighboring N BSs uses one of them. Such division ensures less interference between BSs, at the cost of less intelligent resource allocation. A didactical representation of this scheme is shown in Fig. 5. Using (6) as a reference, each BS v transmits into one specific subchannel m.

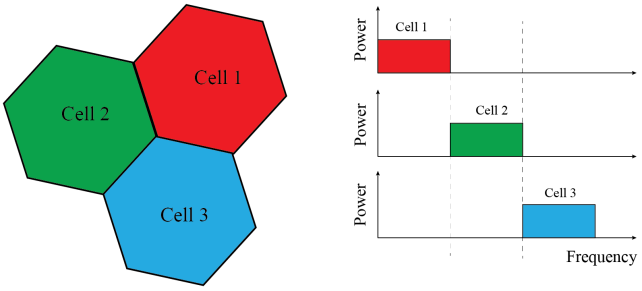

FIGURE 5. Hard FR scheme.

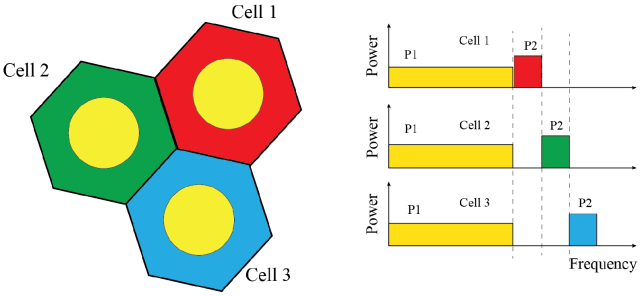

FIGURE 6. Strict FR scheme.

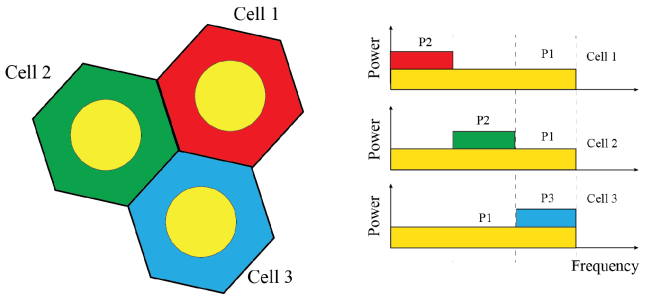

FIGURE 7. Soft FR scheme.

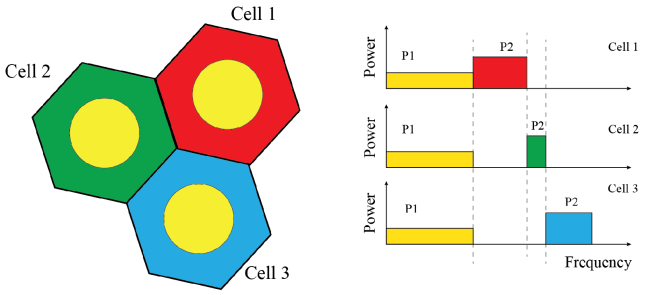

FIGURE 8. Dynamic strict FR scheme.

B. STRICT FREQUENCY REUSE

The band is divided into $N + 1$ subchannels used by all BSs. In each cell-edge, the BSs use a different sub-band to avoid interference. A representation of this scheme is shown in Fig. 6.

Here, the inter-cell interference comes from disjoint sets of the interior subchannel, which is reused by all BSs.

C. SOFT FREQUENCY REUSE

The band is divided into N subchannels; each neighboring BS uses a different subchannel at the edge and center of each cell; thus, the entire band can be used.

Here, a power control $\beta \geq 1$ is considered for the transmit power to generate two different classes: $P_{\text{int}} = p_v^{(t)}$ and $P_{\text{edge}} = \beta p_v^{(t)}$, where P_{int} is the transmit power of the base station if the user y is an interior user, and P_{edge} is the transmit power of the base station if y is a cell-edge user.

The interfering base stations are also divided into two classes: $\mathcal{I}_{\text{int}}$, which consists of all interfering base stations transmitting to cell-interior users on the same subchannel of one specific user with a transmission power of P_{int}, and $\mathcal{I}_{\text{edge}}$, which consists of all interfering base stations transmitting to cell-edge users on the same subchannel with the power transmission P_{edge}.

A heuristic approach proposed in [25] concluded that a typical value of subchannels is between 2 and 20. To accomplish this, a power control factor $\beta \geq 1$ is introduced to the transmit power to create two different classes, P_{int} and P_{edge}, where P_{int} is the transmit power of the base station if the user is an interior user, and P_{edge} is the transmit power of the BS if the user is in the cell-edge network.

A didactic representation of this scheme is shown in Fig. 7.

D. DYNAMIC STRICT REUSE

The algorithm proposed in this Section is based on the Strict FR. Here, the band is also divided into $N+1$ subchannels, but the size of each subchannel is proportional to the number of UEs within the region that each subchannel is serving. Thus, we will refer to this algorithm as Dynamic Strict FR.

To calculate the size of each subchannel, the BSs must communicate with each other in order to discover how many UEs are serving. A representation of this scheme is shown in Fig. 8.

The size ω_i of the edge subchannel of BS i and the size θ of the subchannel in the center of each BS are given by

$$\omega_i = \frac{a_i}{\left(\sum_{i=1}^{n} a_i\right) + b}, \tag{8}$$

and

$$\theta = \frac{b}{\left(\sum_{i=1}^{n} a_i\right) + b}, \tag{9}$$

where a_i is the number of UEs at the edge of BS i, and b is the maximum number of UEs at the center of all BSs.

E. DYNAMICS BASED ON DEEP REINFORCEMENT LEARNING APPROACH

To improve the understanding of this methodology, we expand the explanation into a description of deep reinforcement learning and the particular cost function that is used to maximize the throughput in the following.

Algorithm 1 Algorithm Used in Dynamic Strict FR Scheme

▷ Defining the subchannel bandwidth in the edge and in the cell center.
while Stop Criteria not met **do**
  for i=1 **do** i=i+1
    $b \leftarrow$ number of Users at the center of the cell
    $a_i \leftarrow$ number of Users at the edge
  ▷ Calculating bandwidth for users near the cell center and users in the edge. Iteration in each BS i.
    $\omega_i \leftarrow$ a bandwidth based on the number of users in the edge using Eq. 8.
    $\theta \leftarrow$ a bandwidth based on the number of users in the center of the cell using Eq. 9.
  end for
end while

1) DEEP REINFORCEMENT LEARNING

In machine learning there are three categories; depending on the nature of the information or feedback available to the learning system, these categories are:

- supervised learning;
- unsupervised learning;
- reinforcement learning (RL).

In this paper, we use RL as the approach for optimizing a specific cost function with specific constraints to optimize the system throughput [26], [27]. It is a trial-and-error process where an agent interacts with an unknown environment in a sequence of discrete time steps to achieve a specific target or task. At time t, the agent first observes the current state of the environment, which is a tuple of relevant environment features and denoted by $S^{(t)} \in \mathcal{S}$, where S is a set of possible states. It then takes an action $a^{(t)} \in \mathcal{A}$ from an allowed set of actions $\mathcal{A}$ according to a policy that can be either stochastic, i.e., π with $a^{(t)} \sim \pi(.|\mathcal{S}^{(t)})$ or deterministic, i.e., μ with $a(t) = \mu(\mathcal{S}^{(t)})$. The interactions are modeled as a Markov decision process. For this reason, the environment moves to a next state $S^{(t+1)}$ following an unknown transition matrix that maps state–action pairs onto a distribution of successive states, and the agent receives a reward $S^{(t+1)}$. Overall, the above process is described as an experience at $t+1$ denoted by $e^{(t+1)} = (S^{(t)}, a^{(t)}, r^{(t+1)}, s^{(t+1)})$.

The goal is to learn a policy that maximizes the cumulative discounted reward $R^{(t)}$ at time t, defined as follows:

$$R^{(t)} = \sum_{\tau=0}^{\infty} \gamma^{\tau} r^{(t+\tau+1)}, \text{ and } \gamma \in (0; 1] \tag{10}$$

Owing to the possibility of combining RL with deep learning [28], deep reinforcement learning (DRL) is a highly suitable method for solving problems with a high number of states and low prior knowledge, which is the case of the FR allocation scenario in the available subchannels.

2) COST FUNCTION DEFINITION

Here, we define the radio optimization problem to be optimized. To this end, details of the cost function and its constraints are defined in the following.

The subchannels and power vectors in the time slot t are denoted by $\boldsymbol{\beta}^{(t)} = \left[\beta_{1,1}^{(t)}, \beta_{1,2}^{(t)}, \cdots, \beta_{N,M}^{(t)}\right]^T$ and $\boldsymbol{p}^{(t)} = \left[p_1^{(t)}, \cdots, p_N^{(t)}\right]^T$, respectively. Using (5), we define the sum-rate maximization problem as

$$\begin{aligned} \max_{\boldsymbol{p}^{(t)}, \boldsymbol{\alpha}^{(t)}} & \sum_{n=1}^{N} \mathcal{C}_n^{(t)}(x_i, y_n) \\ \text{s.t. } & 0 \le p_n^{(t)} \le P_{\max}, \quad \forall n \in \mathcal{N}, \\ & \beta_{n,m}^{(t)} \in \{0, 1\}, \quad \forall n \in \mathcal{N}, \ \forall m \in \mathcal{M}, \\ & \sum_{m \in \mathcal{M}} \beta_{n,m}^{(t)} = 1, \quad \forall n \in \mathcal{N}, \end{aligned} \tag{11}$$

where $\mathcal{C}_n^{(t)} = \sum_{m=1}^{M} \mathcal{C}_{n,m}^{(t)}(x_i, y_n)$.

The nonconvex problem in (11) requires a highly complex approach that could also increase the computational complexity. To handle this nonconvex problem, we consider a multiagent learning scheme, where each transmitter, mounted in each BS, operates as an independent learning agent. Each agent successfully executes two policies to determine its associated subchannel and transmission power level. The proposed multiagent approach is easily scalable to more extensive networks and can operate with local information after training.

At the beginning of each time slot, each agent successively executes two policies to determine its associated transmission power level and subchannel. The agents are represented by the BSs, and the environment is the wireless communication channel model in which every agent or BS aims to optimize the network performance based on UEs's location. The DRL considers two different optimizations. The first case, enclosed in the red dotted square in Fig. 9, considers a Critic network and an Actor network [29] (both based on a Deep Q-network) to optimize the stochastic policy that aims to improve the subchannel selection. In the same Figure, a second Deep Q-network, enclosed in the blue dotted square, aims to optimize a second policy; a deterministic policy is used to select a suitable power transmission value. The agent of the second Deep Q-network requires the subchannel decision of the first approach to determine its state input before setting the transmit power of the agent. A brief explanation of the algorithm is detailed in Algorithm 2.

V. SIMULATION

In order to evaluate the traditional FFR algorithms in the OFDMA system operating in 250 MHz, we use the ns-3 simulator, which is widely known and tested by the scientific community [30]. The ns-3 simulator is a discrete event simulator written in open-source C++. In this work, the cellular network module known as LENA [31] is adopted. This ns-3

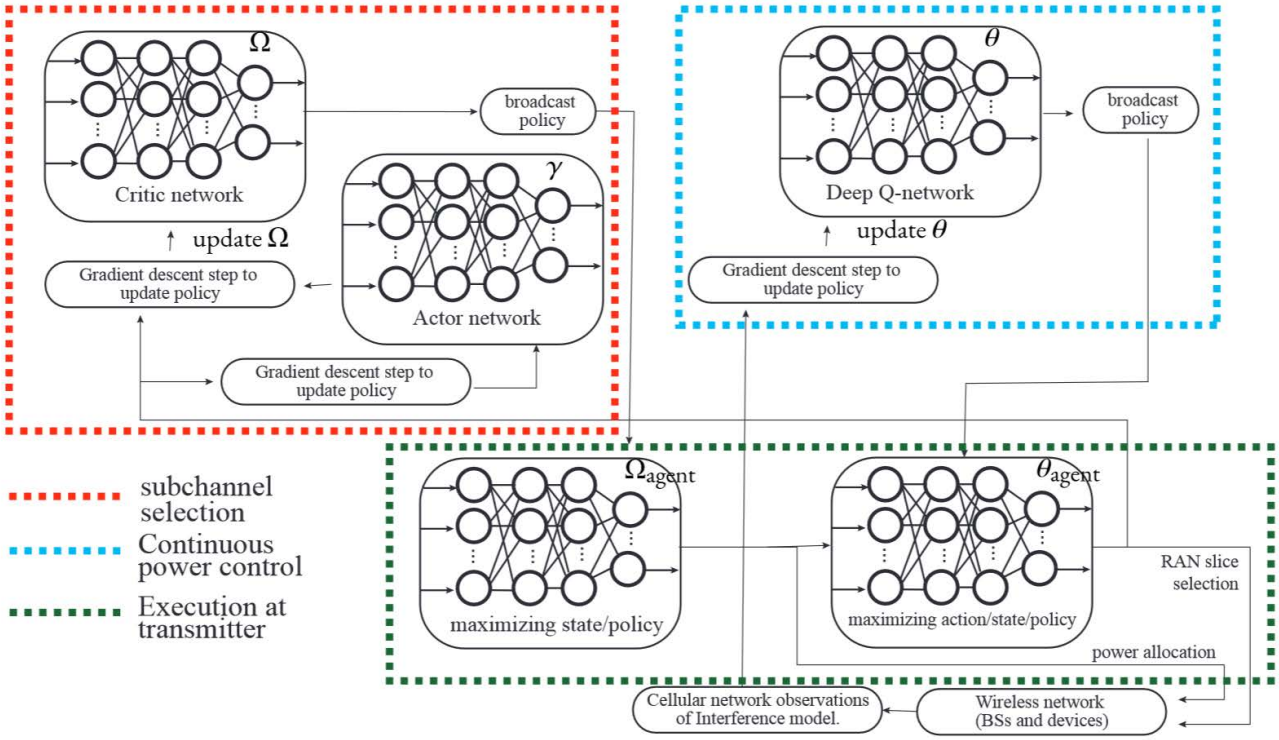

FIGURE 9. Architecture used by the deep reinforcement learning approach in the monte carlo simulation. The reinforcement learning policies Ω, θ, and γ are obtained by using a deep learning gradient descent.

Algorithm 2 Algorithm of the DRL Approach

▷ Main Loop
while Stop Criteria not met **do**
  SUBCHANNEL SELECTION()
  POWER CONTROL()
end while

▷ Subchannel selection
function SUBCHANNEL SELECTION()
  ▷ Agent Selection
  agent $\leftarrow a_n^{(t)} \in \mathcal{A}_{\text{subchannel}} = \{1, \cdots, M\} = \mathcal{M}$
  State set design $\leftarrow s_{n,m}^{(t)}$
  Training by Critic and Actor Network
  Reward function design
  Update Policies: Ω, γ
end function

▷ Power Control
function POWER CONTROL()
  ▷ Agent Selection
  agent $\leftarrow a_{n,a_n^{(t)}}^{(t)} \in \mathcal{A}_{\text{power}} = [0, 1]$
  State set design $\leftarrow s_{n,a_n^{(t)}}^{(t)}$
  Training by deep-Q Network
  Reward function design
  Update Policies: θ
end function

module was chosen in this work because it produces accurate results when compared with commercial devices [32]. To evaluate the DRL model, we use Python and TensorFlow, which is a free and open-source software library for machine learning and artificial intelligence.

Both simulators are adjusted to the parameters described in Table 2 to reflect a real scenario as accurately as possible. The BSs are positioned as shown in Fig. 2, following the same topology as that used in the field. Here, each simulation has a duration of 2.5 s of network time.

The simulations are configured to evaluate the total downlink capacity. Thus, the generated traffic is a constant bit rate (CBR) over the user datagram protocol (UDP) transport protocol.

In order to evaluate the FR algorithms, the UEs are positioned in four different representative scenarios in agribusiness industry:

(I) **UEs on the edge** – Twenty simulations are performed with the UEs positioned at the edge of the cell. Starting with only one UE, each simulation adds a UE for each BS.
(II) **UEs on the center** – The UEs are positioned in the center of the cell in an area of low interference. In the same way as Scenario (I), the number of UEs for each simulation is increased until the number of twenty UEs.
(III) **UEs near to one BS** – Twenty simulations are performed, where eighty UEs are positioned randomly

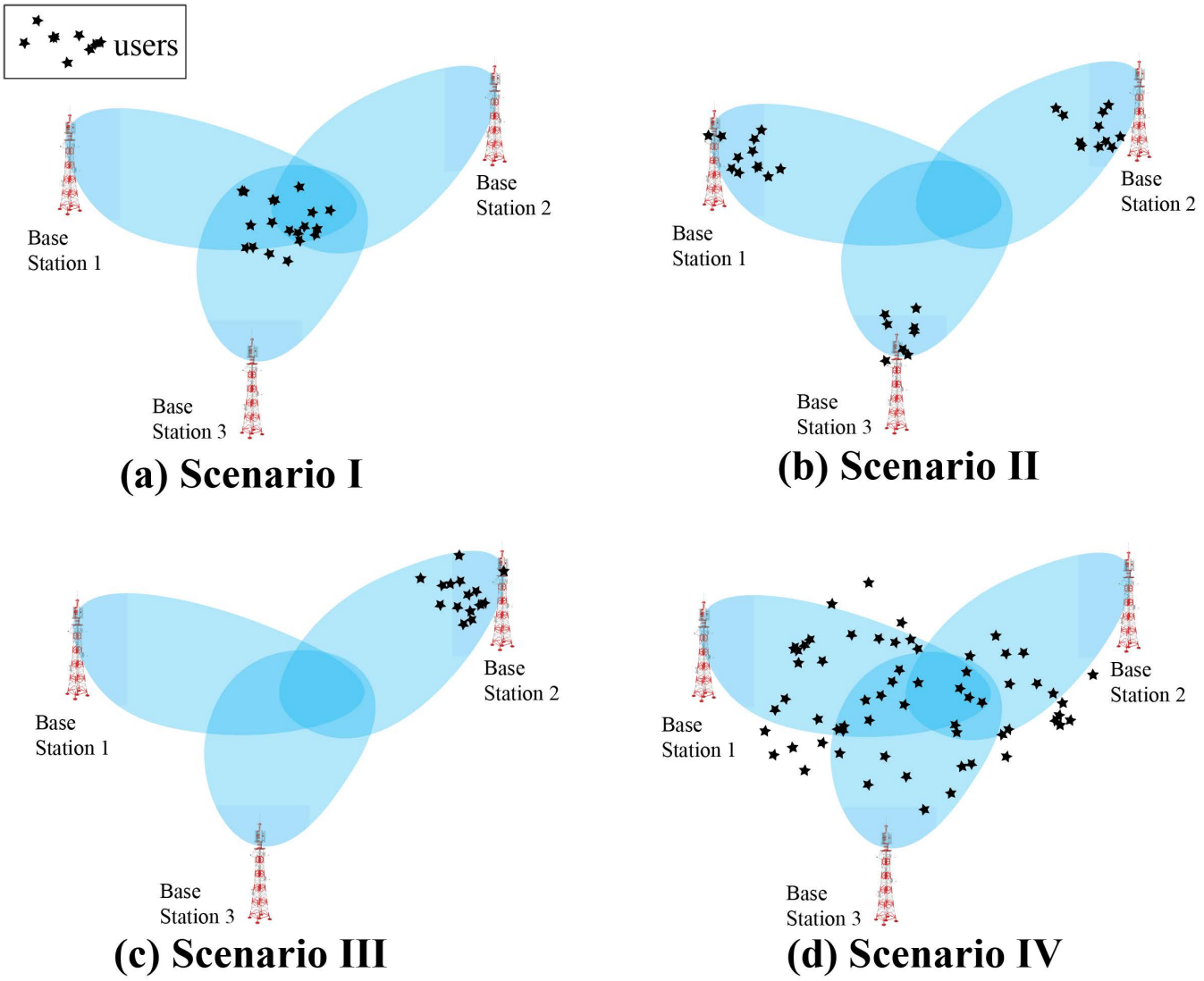

FIGURE 10. Four scenarios evaluated for each FR methodology; in each case, the user distribution is modified based on agribusiness applications.

in a region close to only one BS and connected in that BS.

(IV) **UEs randomly positioned** – One hundred simulations are performed with eighty UEs in the coverage area at random positions and connected to the BS with the best signal.

Scenarios (I), (II), and (III) reflect a situation where the UEs are all positioned close to each other. In the specific application of sugarcane cultivation, this type of scenario reflects a situation in which transport trucks connected to the Internet move together to receive or deliver sugarcane. Such scenarios may reflect other crop and livestock farming applications, such as cattle monitoring in limited pasture areas [33] or precision rotational grazing techniques [34], among other cases.

Scenario (IV) simulates a more generic case with random positioning that aims to analyze the behavior of the system with a large number of UEs.

A graphical representation of these scenarios is given in Fig. 10. Here, we emphasize the radio coverage of the cell radius in each BS. The main aspect of this Figure is the location of users, which is reflected on the final system throughput for each FR scheme.

The performance metrics used to compare these FR methodologies are the following:

- throughput per UE for Scenarios (I), (II), and (III);
- throughput per BS and cumulative distribution function (CDF) for Scenario (IV).

VI. RESULTS

In this Section, the results obtained in all defined scenarios are presented in terms of spectral efficiency to show the learning curve of the methodology based on DRL. After that, the average throughput is obtained for all scenarios defined before.

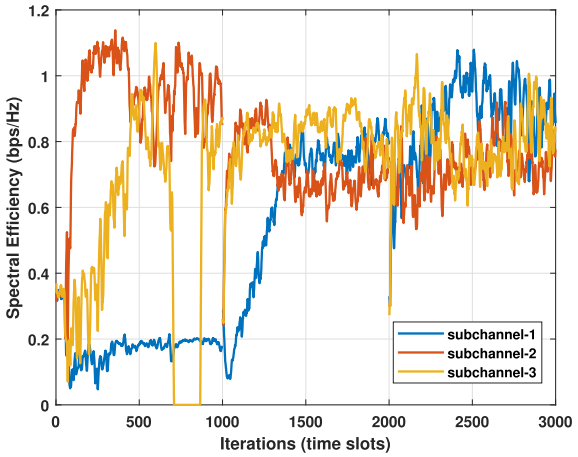

FIGURE 11. Spectral efficiency result in Scenario I when the DRL approach is considered to carry out the FR between three subchannels in the 250 MHz band.

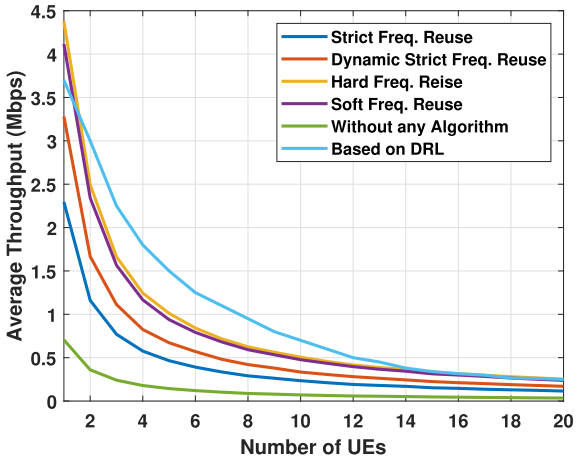

FIGURE 12. Average UE throughput for Scenario (I).

A. DEEP REINFORCEMENT LEARNING APPROACH

Considering a setup defined by Scenario I, the FR based on DRL is evaluated and presented in Fig. 11. The first iterations indicate that the performance of each subchannel is very low. However, when the number of iterations is increased, the deep-Q network and the policies provide better resource allocation, with a gain of 5 compared with the spectral efficiency in iteration 10 and iteration 25000.

It is important to remark that the spectral efficiency is combined with the bandwidth defined in Table 2 to obtain the throughput, which is used in the next results.

B. SCENARIO I

Fig. 12 shows the results of the simulations for the throughput per UE in Scenario (I). In this case, the high interference limits the performance of the system, reducing the throughput of the UEs. When all UEs are in a region of high interference, the FR based on DRL achieves a better performance when compared with the traditional FR schemes. However, the *Hard FR algorithm* presents the best performance when there are two or fewer users to be served. Because the methodology *based on DRL* optimizes the subchannel and power transmission allocation per UE, it has a better performance when the number of UEs is greater than 2. This performance remains until the number of UEs is lower than 14 simultaneous users. Because the *Hard FR* divides the spectrum for each BS, this algorithm is the second best methodology that guarantees less interference but with no flexibility for changes in spectrum allocation. The *Soft FR* technique performs very close to *Hard FR* because the UEs are located on the border of the cell, and the division of the subchannels is done in the same way as the *Hard FR*. However, the *Soft FR* algorithm has the advantage of greater flexibility in the allocation of RBs, in case the UEs are in a situation of lower interference. The *Dynamic Strict FR* algorithm also divides the subchannels like the other two algorithms after some parameter calculation defined in (8) and (9). However, its performance is close to the *Soft FR* technique. The *Strict FR* technique presents a less satisfactory performance because it reserves only part of the available band to the UEs on the edge of the cell. Finally, as expected, using no algorithm is the worst choice because resources are not being used efficiently under the high interference scenario.

C. SCENARIO II

When all UEs are in a situation of less interference (Scenario (II)), the results indicate that there is no need for any FR algorithm. In this scenario, not using any algorithm is the alternative that guarantees the highest throughput, because the UEs can transmit over the entire band with a very low probability of inter-cell interference, as it is shown in Fig. 13. We also note that the *Soft FR* technique outperforms similarly because it allows the BSs to use the entire band in the middle of the cell. By reserving a subchannel for the UEs with more significant interference, the algorithm of *Strict FR* shows a poor performance. The *Hard FR* algorithm divides the band between BSs, reducing its performance. The *Dynamic Strict FR* technique presents an intermediary performance because of its time for calculating the proper quantity of RBs for each BS. The methodology *based on DRL* achieves a similar performance to the *Dynamic Strict FR* when the number of simultaneous UEs is smaller than eight. However, when the number of UEs is increased, the performance tends to improve the average throughput.

D. SCENARIO III

When all UEs are connected to the same BS (Scenario (III)), the result is similar to Scenario (II), i.e., a scenario with a very low probability of interference. As the *Hard FR* and the *Strict FR* algorithms reserve a specific subchannel in each BS that is not serving any user, both show an inefficient use of the available resources, which explains their poor performance. As presented in Fig. 14, the *Soft FR*, the *Dynamic Strict FR*, the no-algorithm use case, and the FR based on DRL achieve a better performance without any significant difference.

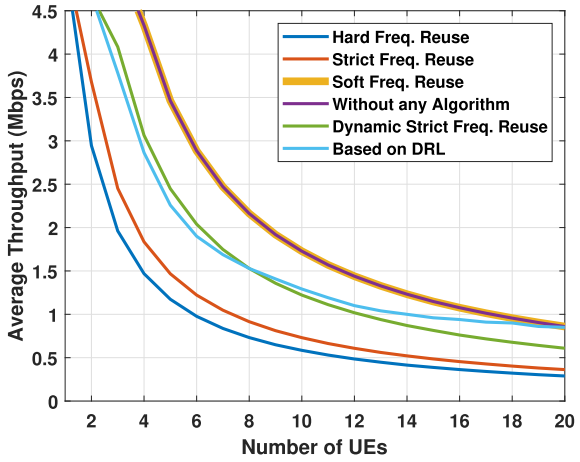

FIGURE 13. Average UE throughput in Scenario (II).

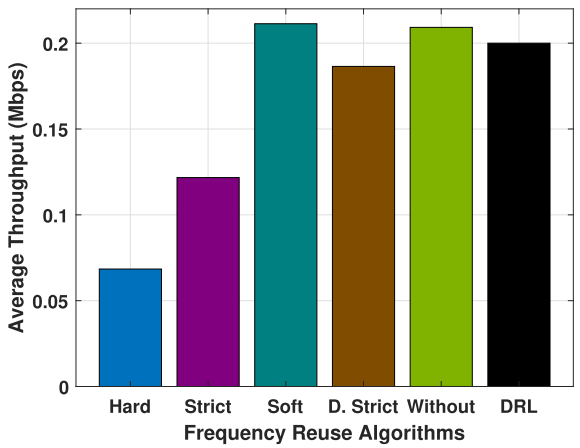

FIGURE 14. Average UE throughput for Scenario (III).

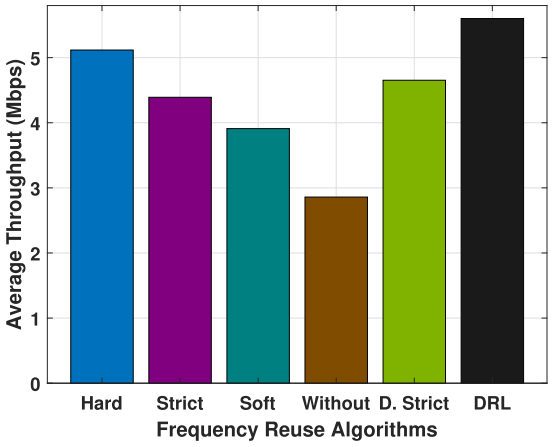

FIGURE 15. Average throughput for Scenario (IV).

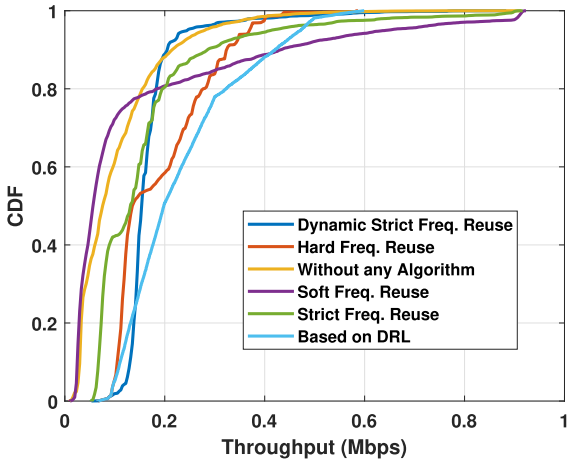

FIGURE 16. CDF of throughput for Scenario (IV).

E. SCENARIO IV

The results of the simulation campaign for Scenario (IV) are shown in Figs. 15 and 16 to represent the throughput and the cumulative distribution function of the UE throughput per BS, respectively. In general, in this scenario it is always convenient to use some FR methodology. However, as the UEs are positioned randomly using a uniform distribution, the FR based on DRL outperforms the other traditional methodologies.

We can see in Fig. 15 that in the 60% percentile of the measurements, the hard FR and the methodology based on DRL achieves a better throughput than the other traditional methodologies. However, as we analyze Fig. 16, we observe that the great part of UEs (almost 60%) have a throughput very close to zero (less than 0.1 Mbps).

As the *Soft FR* algorithm allows all cells to use the entire band in the center, the interference increases for UEs in the transition region between the cell center and the cell border. A result of this is that approximately 70% of the UEs have an average throughput below 0.1 Mbps. It can be verified that the average throughput of 40% of the UEs is below 0.1 Mbps when the Strict FR technique is adopted. The *Dynamic Strict FR* algorithm provides a higher fairness between the UEs, as approximately 90% of the UEs have an average throughput between 0.1 and 0.2 Mbps. Finally, the CDF indicates that the performance of the algorithm, which is based on DRL, outperforms the other traditional methodologies.

VII. CONCLUSION

The need for IoT applications in agribusiness has driven the development of cellular broadband systems using sub-1GHz bands owing to the long-range transmission required by connectivity in rural areas. However, the propagation in such bands implies an increase in interference, which usually degrades the system performance.

This work compared the performance of a cellular network using traditional FR schemes with a data-driven approach based on DRL when the system is operating in 250 MHz, which is a band not yet standardized and which has received limited attention in the literature so far. The simulation tools were calibrated using data gathered in drive test sessions using a real cellular network operating in the 250 MHZ band.

Thus, the results of this work provide a strong ground because they are obtained considering a real setup as a benchmark.

Four scenarios were defined to represent typical agribusiness setups in terms of UE distribution. In Scenarios I and IV, the approach based on DRL achieves a better performance than the traditional FR schemes. In Scenarios II and III, the cellular system performance reaches a better performance when no FR methodology is considered. However, the approach based on DRL improves its performance when the number of simultaneous connected UEs is increased.

A. FINAL REMARKS

The importance of using machine learning schemes on FR allocation is an attractive approach, especially in methodologies that aim to maximize the allocation of resources in high-interference scenarios. A widespread scenario in agribusiness applications is the grouping of UEs in a cell region, either at the edge or center of the cell. The gain of using fractional reuse techniques is apparent when the analysis is performed with UEs located at the edges of the cells (Scenario (I)). For instance, in a system with four UEs per cell in Scenario I, the average throughput per UE increased from 0.15 Mbps to 1.13 Mbps when using the *Hard FR* or *Soft FR* algorithm when compared with a scenario that did not use any FR scheme. A similar comparison between the methodology based on DRL and not using any algorithm indicates that the average throughput is increased from 0.15 Mbps to 1.83 Mbps. In practice, it means that the UE can support video services (throughput over 800 kbps) instead of just supporting telemetry services (over 100 kbps) when any FR scheme is used.

When the agribusiness application requires fairness, i.e., all UEs with a minimum throughput, the FR based on DRL is the most acceptable alternative in high-interference scenarios, such as Scenario (IV). The methodology performs satisfactorily in low-interference scenarios when the number of simultaneous users is increased, such as in Scenario (III).

B. FUTURE WORK

The paper suggests that a similar DRL approach can be handled on 5G New Radio operating in sub-6GHz, specifically in the evolution of 5G-Advanced, which is standardized by the 3GPP Rel. 18.

Other interesting topic of future work would be to analyze beyond 5G networks to compare the performance of cell-free massive MIMO [35] in rural scenarios with the schemes proposed in this paper.

REFERENCES

[1] Y. Siriwardhana, C. De Alwis, G. Gür, M. Ylianttila, and M. Liyanage, "The fight against the COVID-19 pandemic with 5G technologies," *IEEE Eng. Manag. Rev.*, vol. 48, no. 3, pp. 72–84, Sep. 2020.

[2] A. M. Cavalcante, P. H. Gomes, M. V. Marquezini, I. Bonomini, and L. L. Mendes, "Applicability of IoT technologies for 5G use cases in Brazil," in *Proc. IEEE 2nd 5G World Forum (5GWF)*, Sep. 2019, pp. 53–57.

[3] M. S. Hossain, G. Muhammad, and N. Guizani, "Explainable AI and mass surveillance system-based healthcare framework to combat COVID-I9 like pandemics," *IEEE Netw.*, vol. 34, no. 4, pp. 126–132, Jul. 2020.

[4] D. Carrillo and J. Seki, "Rural area deployment of Internet of Things connectivity: LTE and LoRaWAN case study," in *Proc. IEEE 24th Int. Conf. Electron., Electr. Eng. Comput. (INTERCON)*, Aug. 2017, pp. 1–4.

[5] Y. Wei and S.-H. Hwang, "Investigation of spectrum values in rural environments," *ICT Exp.*, vol. 4, no. 4, pp. 234–238, Dec. 2018.

[6] V. S. Anusha, G. K. Nithya, and S. N. Rao, "Comparative analysis of wireless technology options for rural connectivity," in *Proc. IEEE 7th Int. Advance Comput. Conf. (IACC)*, Jan. 2017, pp. 402–407.

[7] A. Jha and D. Saha, "Techno-economic assessment of the potential for LTE based 4G mobile services in rural India," in *Proc. IEEE Int. Conf. Adv. Netw. Telecommun. Syst. (ANTS)*, Dec. 2015, pp. 1–6.

[8] C. Ovando, J. Pérez, and A. Moral, "LTE techno-economic assessment: The case of rural areas in Spain," *Telecommun. Policy*, vol. 39, nos. 3–4, pp. 269–283, May 2015.

[9] A. S. Yogapratama, U. K. Usman, and T. A. Wibowo, "Analysis on 900 MHz and 1800 MHz LTE network planning in rural area," in *Proc. 3rd Int. Conf. Inf. Commun. Technol. (ICoICT)*, May 2015, pp. 135–139.

[10] M. Lauridsen, I. Z. Kovacs, P. Mogensen, M. Sorensen, and S. Holst, "Coverage and capacity analysis of LTE-M and NB-IoT in a rural area," in *Proc. IEEE 84th Veh. Technol. Conf. (VTC-Fall)*, Sep. 2016, pp. 1–5.

[11] M. Lauridsen, L. C. Gimenez, I. Rodriguez, T. B. Sorensen, and P. Mogensen, "From LTE to 5G for connected mobility," *IEEE Commun. Mag.*, vol. 55, no. 3, pp. 156–162, Mar. 2017.

[12] P. Gawlowicz, N. Baldo, and M. Miozzo, "An extension of the ns-3 LTE module to simulate fractional frequency reuse algorithms," in *Proc. Workshop ns (WNS)*, 2015, pp. 98–105.

[13] A. S. Hamza, S. S. Khalifa, H. S. Hamza, and K. Elsayed, "A survey on inter-cell interference coordination techniques in OFDMA-based cellular networks," *IEEE Commun. Surveys Tuts.*, vol. 15, no. 4, pp. 1642–1670, 4th Quart., 2013.

[14] S. Sadr, A. Anpalagan, and K. Raahemifar, "Radio resource allocation algorithms for the downlink of multiuser OFDM communication systems," *IEEE Commun. Surveys Tuts.*, vol. 11, no. 3, pp. 92–106, 3rd Quart., 2009.

[15] V. Fernández-López, K. I. Pedersen, and B. Soret, "Interference characterization and mitigation benefit analysis for LTE-A macro and small cell deployments," *EURASIP J. Wireless Commun. Netw.*, vol. 2015, no. 1, pp. 1–12, Dec. 2015.

[16] B. Bojović, E. Meshkova, N. Baldo, J. Riihijärvi, and M. Petrova, "Machine learning-based dynamic frequency and bandwidth allocation in self-organized LTE dense small cell deployments," *EURASIP J. Wireless Commun. Netw.*, vol. 2016, no. 1, pp. 1–16, Dec. 2016.

[17] S. Gimenez, D. Martín-Sacristán, D. Calabuig, and J. F. Monserrat, "Self-configurable coordinated scheduling for ultra-dense small cell deployments," in *Proc. 13th Int. Wireless Commun. Mobile Comput. Conf. (IWCMC)*, Jun. 2017, pp. 512–517.

[18] C. Feijóo, J.-L. Gómez-Barroso, and S. Ramos, "An analysis of next generation access networks deployment in rural areas," in *Proc. 50th FITCE Congr.-ICT, Bridging Ever Shifting Digit. Divide*, Aug. 2011, pp. 1–18.

[19] Z. Wang, J. Zong, Y. Zhou, Y. Shi, and V. W. Wong, "Decentralized multi-agent power control in wireless networks with frequency reuse," *IEEE Trans. Commun.*, vol. 70, no. 3, pp. 1666–1681, Mar. 2022.

[20] J. Zhao, Y. Zhang, Y. Nie, and J. Liu, "Intelligent resource allocation for train-to-train communication: A multi-agent deep reinforcement learning approach," *IEEE Access*, vol. 8, pp. 8032–8040, 2020.

[21] E. B. Perri and L. C. Trintinalia, "Secondary lobe level control in antenna arrays," in *Proc. SBMO/IEEE MTT-S Int. Microw. Optoelectron. Conf. (IMOC)*, vol. 2, Sep. 2003, pp. 845–850 vol. 2.

[22] *Resolução no 555, de 20 de Dezembro de 2010*, Agência Nacional de Telecomunicações (ANATEL), Brasília, Brazil, Dec. 2010.

[23] *Technical Specification Group Radio Access Network; E-UTRA and E-UTRAN; Overall Description*, document 3GPP TS 36.300, 3GPP LTE Release 8. Accessed: Apr. 2018. [Online]. Available: http://www.3gpp.org/specifications/releases/72-release-8

[24] A. Medeisis and A. Kajackas, "On the use of the universal Okumura-Hata propagation prediction model in rural areas," in *Proc. IEEE 51st Veh. Technol. Conf. (VTC-Spring)*, vol. 3, May 2000, pp. 1815–1818.

[25] T. Novlan, R. Ganti, A. Ghosh, and J. Andrews, "Analytical evaluation of fractional frequency reuse for OFDMA cellular networks," *IEEE Trans. Wireless Commun.*, vol. 10, no. 12, pp. 4294–4305, Dec. 2011.

[26] V. François-Lavet, P. Henderson, R. Islam, M. G. Bellemare, and J. Pineau, *An Introduction to Deep Reinforcement Learning*. Boston, MA, USA: Now, 2018.

[27] M. Kenyeres and J. Kenyeres, "Comparative study of distributed consensus gossip algorithms for network size estimation in multi-agent systems," *Future Internet*, vol. 13, no. 5, p. 134, May 2021.
[28] M. Morales, *Grokking Deep Reinforcement Learning*. Shelter Island, NY, USA: Manning Publications, 2020.
[29] Q. Wei, L. Wang, Y. Liu, and M. M. Polycarpou, "Optimal elevator group control via deep asynchronous actor–critic learning," *IEEE Trans. Neural Netw. Learn. Syst.*, vol. 31, no. 12, pp. 5245–5256, Dec. 2020.
[30] NS-3. *Network Simulator-3*. Accessed: Apr. 2018. [Online]. Available: https://www.nsnam.org/
[31] N. Baldo, M. Miozzo, M. Requena-Esteso, and J. Nin-Guerrero, "An open source product-oriented LTE network simulator based on ns-3," in *Proc. 14th ACM Int. Conf. Modeling, Anal. Simulation Wireless Mobile Syst. (MSWiM)*, 2011, pp. 293–298.
[32] A. Marinescu, I. Macaluso, and L. A. DaSilva, "System level evaluation and validation of the ns-3 LTE module in 3GPP reference scenarios," in *Proc. 13th ACM Symp. QoS Secur. Wireless Mobile Netw. (Q2SWinet)*. New York, NY, USA: Association for Computing Machinery, 2017, pp. 59–64, doi: 10.1145/3132114.3132117.
[33] M. L. Chizzotti, F. S. Machado, E. E. L. Valente, L. G. R. Pereira, M. M. Campos, T. R. Tomich, S. G. Coelho, and M. N. Ribas, "Technical note: Validation of a system for monitoring individual feeding behavior and individual feed intake in dairy cattle," *J. Dairy Sci.*, vol. 98, no. 5, pp. 3438–3442, May 2015. [Online]. Available: http://www.sciencedirect.com/science/article/pii/S0022030215001794
[34] D. P. Eaton, S. A. Santos, M. D. C. A. Santos, J. V. B. Lima, and A. Keuroghlian, "Rotational grazing of native pasturelands in the pantanal: An effective conservation tool," *Tropical Conservation Sci.*, vol. 4, no. 1, pp. 39–52, Mar. 2011, doi: 10.1177/194008291100400105.
[35] E. Björnson and L. Sanguinetti, "Making cell-free massive MIMO competitive with MMSE processing and centralized implementation," *IEEE Trans. Wireless Commun.*, vol. 19, no. 1, pp. 77–90, Jan. 2020.

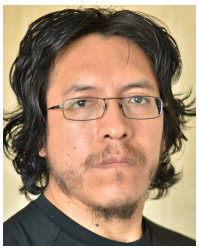

DICK CARRILLO MELGAREJO (Member, IEEE) received the B.Eng. degree (Hons.) in electronics and electrical engineering from San Marcos National University, Lima, Perú, and the M.Sc. degree in electrical engineering from the Pontifical Catholic University of Rio de Janeiro, Brazil, in 2004 and 2008, respectively. He is currently pursuing the Ph.D. degree in electrical engineering with LUT University. Since 2018, he has been a Researcher at LUT University. His research interests include mobile technologies beyond 5G, RAN slicing, and machine learning in wireless communication.

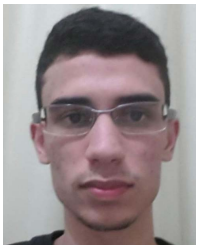

LUIZ QUIRINO REZENDE DA COSTA FILHO is currently pursuing the B.Eng. degree in electrical engineering with the Federal University of Juiz de Fora. His research interests include wireless networks, sensor networks, and network simulation.

ÁLVARO AUGUSTO MACHADO DE MEDEIROS received the B.Sc. degree in electrical engineering from the Federal University of Rio Grande do Norte, Brazil, in 2000, and the M.Sc. and Ph.D. degrees in electrical engineering from the University of Campinas, Brazil, in 2002 and 2007, respectively. From 2007 to 2010, he was a Research Specialist with the Nokia Institute of Technology, Brazil, and the Research and Development Center, Brazil. Since 2010, he has been with the Federal University of Juiz de Fora, Brazil, where he is currently an Associate Professor. In 2021, he joined as a Postdoctoral Researcher with Munster Technological University, Cork, Ireland. His research interests include wireless communications, wireless channel modeling, medium access control, and wireless system dimensioning and performance analysis.

CARLOS LORENA NETO was born in Campinas, Brazil, in 1973. He received the B.S. degree in electrical engineering from the Universidade Estadual de Campinas—UNICAMP, Campinas, Brazil, in 1996. Since 1996 he is working as a Professional Engineer in the area of telecommunications, wireless communications, and machine learning. He is currently the Senior System Engineer in wireless and machine learning with Tropico Sistemas e Telecomunicacoes SA.

FABRICIO LIRA FIGUEIREDO received the degree in electronics engineering from the Federal University of Pernambuco (UFPE), in 1995, and the M.Sc. degree in electrical engineering and the Ph.D. degree in wireless communications area from the State University of Campinas (UNICAMP), in 1999 and 2008, respectively. He is currently the Smart Agribusiness Manager of CPqD, leading CPQD business and innovation strategy targeting rural and remote areas. He has been the Manager of the Wireless Communications Division, CPQD, from 2008 to 2017. His research interests include mobile broadband networks, IoT connectivity, intelligent antennas, cognitive radio, self-organizing networks, machine learning, and speech recognition.

DEMÓSTENES ZEGARRA RODRÍGUEZ (Senior Member, IEEE) received the B.Sc. degree in electronic engineering from the Pontifical Catholic University of Peru, and the M.S. and Ph.D. degrees from the University of São Paulo, in 2009 and 2013, respectively. He is currently an Adjunct Professor with the Department of Computer Science, Federal University of Lavras, Brazil. He has a solid knowledge in telecommunication systems and computer science based on 15 years of professional experience in major companies. His research interests include QoS and QoE in multimedia services, architect solutions in telecommunication systems, artificial intelligence algorithms, and online social networks.